ADVANCED THERAPEUTICS
www.advtherap.com

X-Ray Co-Crystal Structure Guides the Way to Subnanomolar Competitive Ecto-5′-Nucleotidase (CD73) Inhibitors for Cancer Immunotherapy

Sanjay Bhattarai, Jan Pippel, Anne Meyer, Marianne Freundlieb, Constanze Schmies, Aliaa Abdelrahman, Amelie Fiene, Sang-Yong Lee, Herbert Zimmermann, Ali El-Tayeb, Gennady G. Yegutkin, Norbert Sträter, and Christa E. Müller**

Ecto-5′-nucleotidase (CD73, EC 3.1.3.5) catalyzes the extracellular hydrolysis of AMP yielding adenosine, which induces immunosuppression, angiogenesis, metastasis, and proliferation of cancer cells. CD73 inhibition is therefore proposed as a novel strategy for cancer (immuno)therapy, and CD73 antibodies are currently undergoing clinical trials. Despite considerable efforts, the development of small molecule CD73 inhibitors has met with limited success. To develop a suitable drug candidate, a high resolution (2.05 Å) co-crystal structure of the CD73 inhibitor PSB-12379, a nucleotide analogue, in complex with human CD73 is determined. This allows the rational design and development of a novel inhibitor (PSB-12489) with subnanomolar inhibitory potency toward human and rat CD73, high selectivity, as well as high metabolic stability. A co-crystal structure of PSB-12489 with CD73 (1.85 Å) reveals the interactions responsible for increased potency. PSB-12489 is the most potent CD73 inhibitor to date representing a powerful tool compound and novel lead structure.

Adenosine is one of the strongest immunosuppressive agents of the innate immune system by activating G protein-coupled adenosine A_{2A} and A_{2B} receptors.[1] In addition to mediating immune escape, adenosine stimulates angiogenesis, metastasis, and proliferation of cancer.[1,2] Large amounts of extracellular adenosine are produced by cancer cells through the up-regulation of ecto-5′-nucleotidase (CD73, EC 3.1.3.5), which catalyzes the hydrolysis of adenosine-5′-monophosphate (AMP). CD73 is a ≈140 kDa Zn^{2+}-binding glycosylphosphatidylinositol-anchored homodimeric membrane protein.[3] It can also be cleaved and released as a soluble enzyme,[4] whose crystal structure has been published (pdb: 4H2I).[5]

CD73 was recently proposed as a novel drug target for the (immuno)therapy of cancer,[2,6,7] and antibodies against CD73 are currently evaluated in clinical trials.[8] However, those antibodies typically show only partial inhibition of CD73, and moreover, they may not penetrate well into solid tumors. Thus, small molecule CD73 inhibitors would be superior for therapeutic application. However, despite considerable efforts, only few inhibitors have been reported so far[9–15] and most of them appear unsuitable for in vivo application due to low potency, low selectivity, metabolic instability, low water-solubility, and/or high plasma protein binding.[16]

In a quest to develop suitable candidates, we selected the moderately potent competitive CD73 inhibitor **1**, α,β-Methylene-ADP [AOPCP (**1**)], a more stable analog of the natural inhibitor adenosine diphosphate (ADP), as lead structure. Substitution of

Dr. S. Bhattarai, Dr. A. Meyer, Dr. M. Freundlieb, C. Schmies, Dr. A. El-Tayeb, Dr. A. Abdelrahman, Dr. A. Fiene, Dr. S.-Y. Lee, Prof. C. E. Müller
PharmaCenter Bonn, Pharmaceutical Institute
Department of Pharmaceutical & Medicinal Chemistry
University of Bonn
An der Immenburg 4, D-53121 Bonn, Germany
E-mail: christa.mueller@uni-bonn.de

Dr. J. Pippel, Prof. N. Sträter
Institute of Bioanalytical Chemistry
Center for Biotechnology and Biomedicine
Leipzig University
Deutscher Platz 5, 04103 Leipzig, Germany
E-mail: strater@bbz.uni-leipzig.de

Prof. H. Zimmermann
Institute of Cell Biology and Neuroscience
Goethe-University
Frankfurt am Main, Germany

Dr. G. G. Yegutkin
Medicity Research Laboratory
University of Turku
20520 Turku, Finland

The ORCID identification number(s) for the author(s) of this article can be found under https://doi.org/10.1002/adtp.201900075

DOI: 10.1002/adtp.201900075

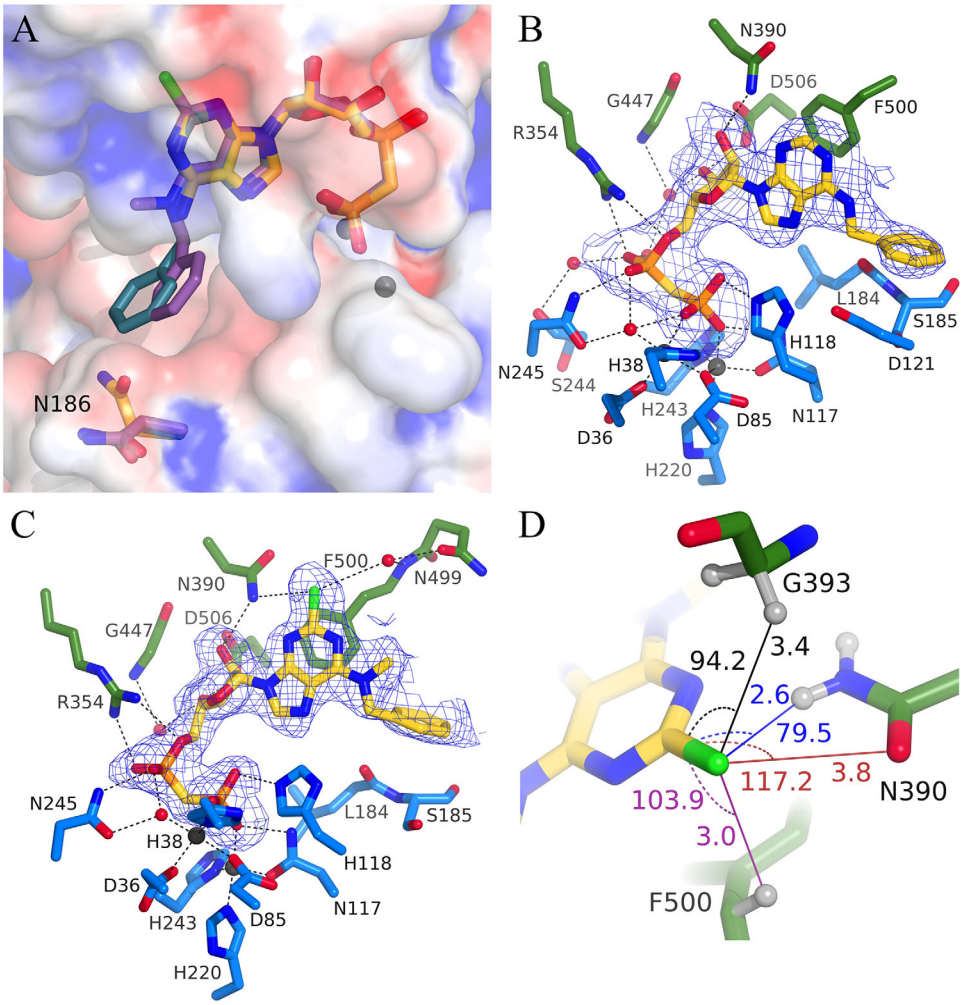

Figure 1. A) Binding modes of PSB12379 (**2**) and PSB12489 (**5**) to human CD73. Superposition of AOPCP (yellow, pdb code: 4H2I), PSB12379 (turquoise), and PSB12489 (purple) bound to CD73 (molecular surface colored by electrostatic potential). Interactions of B) PSB12379 and C) PSB12489 within the substrate binding site formed by the N-terminal (blue) and C-terminal (green) domains. Difference electron density omit maps (contoured at 2.0 σ) are shown in blue. D) Close-up of the interactions of the chloro substituent (green) in PSB12489. Distances (in Å) and angles (°) are indicated. The NH group of N390 is positioned for a favorable side-on interaction with the chloro substituent. The carbonyl oxygen of N390 is too far away from a linear C—Cl···O arrangement for a halogen bonding interaction.

the adenine core and modification of the ribose and diphosphate moieties revealed initial structure–activity relationships.[17] Pyrimidine analogs of **1** were also evaluated, but were generally less potent than corresponding purine derivatives, and their selectivity versus P2Y nucleotide receptors was mostly moderate.[18] N^6-benzyladenosine-5′-*O*-[(phosphonomethyl)phosphonic acid] (**2**, PSB-12379, K_i 9.03 nM) was discovered by our group as a more potent inhibitor than **1**,[17] and **2** is now widely employed as a (commercially available) tool compound. One of its drawbacks is the potential hydrolysis of the 5′-phosphonic acid ester resulting in the formation of N^6-benzyladenosine, which is an agonist of adenosine receptors and would thus result in undesired effects. In the present study, we describe the preparation of a co-crystal structure of inhibitor **2** with human CD73. This first structure of CD73 in complex with a potent inhibitor was utilized to design significantly improved inhibitors. Finally, we obtained an additional co-crystal structure of the optimized CD73 inhibitor **5** to evaluate our design hypothesis and to explain its improved potency.

The co-crystal structures of human CD73 in the closed state with compound **2** (PSB-12379) and **5** (PSB-12489) was obtained by crystallizing the protein in the presence of 100 µM Zn^{2+} and the respective inhibitor in analogy to Knapp et al.[5] For both data sets, relatively high-resolution limits were achieved, and thus well-defined electron densities for the inhibitors and the two Zn^{2+} ions were obtained in the active site. These co-crystal structures allow for a rational explanation of the inhibitory potency improvements on a structural level (Table S1, Supporting Information). Previously described inhibitor **2** (PSB-12379) showed an ≈40-fold improved K_i-value compared to AOPCP (**1**).[17] AOPCP binds to the closed conformation of CD73 with the adenine base forming a hydrophobic stacking interaction with F417 and F500 of the specificity pocket in the C-terminal domain, whereas the terminal phosphate group is coordinated

Table 1. Potency of inhibitors at rat and human CD73.

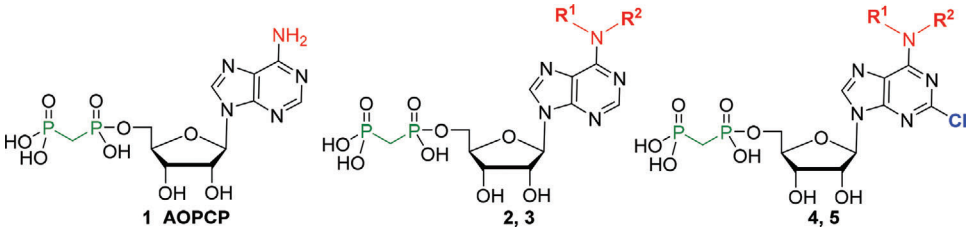

Compd.	R^1	R^2	rat CD73 $K_i \pm$ SEM [nM]	human CD73 $K_i \pm$ SEM [nM]
1[17] (AOPCP)	See structure above		**197** ± 5	**88.4** ± 4.0
2[17] (PSB-12379)	Benzyl	H	**9.03** ± 1.24	
3 (PSB-12437)	Benzyl	Methyl	**4.64** ± 0.23	
4 (PSB-12651)	Benzyl	H	**1.23** ± 0.04	
5 (PSB-12489)	Benzyl	Methyl	**0.746** ± 0.246	0.318 ± 0.020

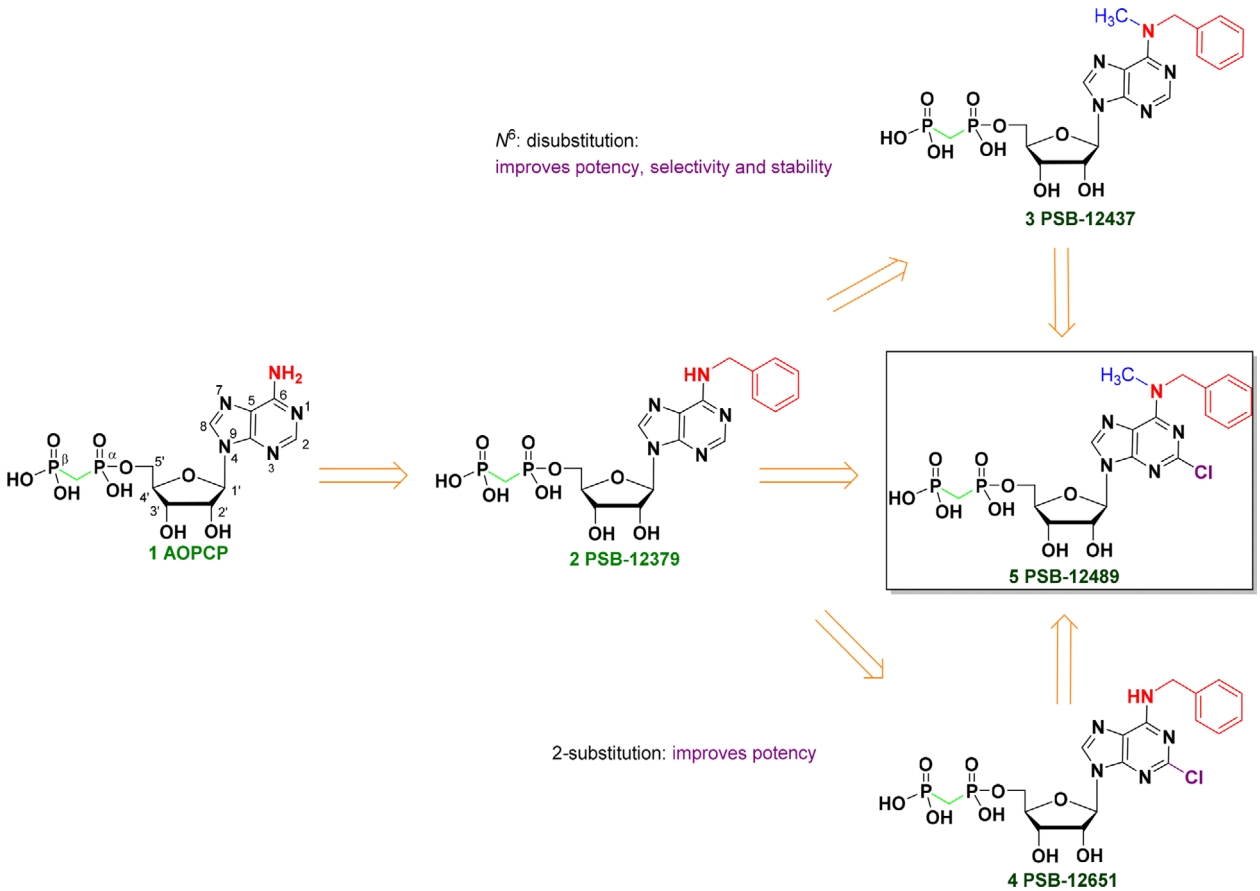

Figure 2. Schematic design of the inhibitor **5** based on the co-crystal structure of **2** with human CD73. Addition of an exocyclic methyl group at the N^6-position to lock the conformation of **2** resulted in **3**. N^6,N^6-di-substituted derivatives will not yield adenosine receptor-activating metabolites. Addition of a chloro substituent at position 2 of the adenine core structure resulted in **4**, based on the rationale to trap an additional water-filled cavity of ≈210 Å^3. PSB-12489 (**5**) was designed by combining the improved features of **3** and **4**.

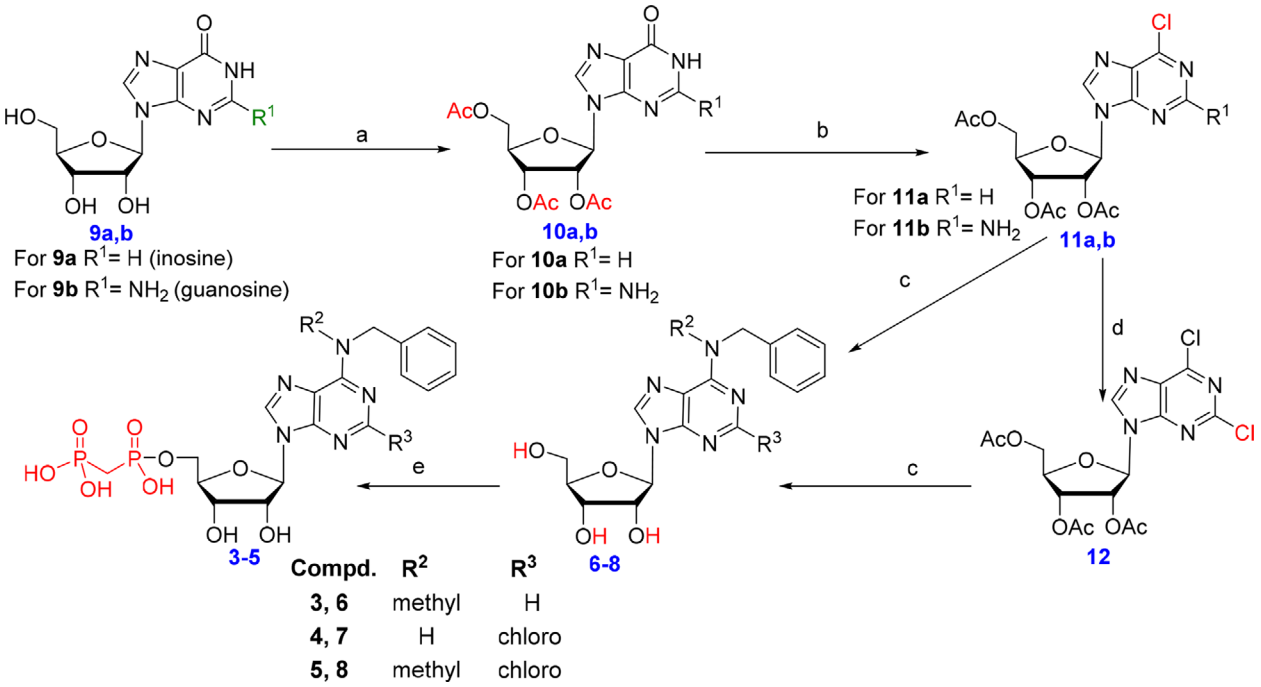

Scheme 1. Synthesis of 2- and N^6-substituted purine riboside-5′-*O*-[(phosphonomethyl)phosphonic acid] derivatives. Reagents and conditions: a) Acetic anhydride, dimethylaminopyridine (DMAP), ethyl(dimethyl)amine (EDMA), 40 °C, 1 h, yield 97%; b) $POCl_3$, *N*,*N*-dimethylaniline, TEAC, reflux, 110 °C, 15 min, yield 75%; c) two steps: i) benzylamine or methyl-1-phenylmethanamine, triethylamine, absolute ethanol, reflux, 60 °C, 4 h, yield 95%, ii) 2% $NaOCH_3$ in methanol, rt, 24 h, yield 70%; d) benzyltriethylammonium nitrite, acetyl chloride, dichloromethane (DCM), 2 h, yield 70%; e) two steps: i) methylenebis(phosphonic dichloride), trimethyl phosphate, 4 °C, 40 min, ii) TEAC buffer pH 7.4–7.6, rt, 15 min, yield 60–70%. For detailed synthetic procedure, see Supporting Information.

to the two catalytic zinc ions of the N-terminal domain.[5] This binding mode is maintained for **2** (**Figure 1**). In addition, positions of residues in spatial proximity to the active site of CD73 also remain unchanged, except for N186 which is shifted to provide space for the N^6-benzyl substituent. The benzyl moiety forms hydrophobic interactions with the N-terminal domain involving the carbon atoms of D121, S185, and N186 (Figure 1). The benzyl group exhibits weaker electron density and higher Debye-Waller factor (B-values) compared to the core structure of **2**, indicating a greater flexibility of this group.

To further improve the inhibitory potency of **2**, combinations of the N^6-benzyl substituent with an additional alkyl group at the exocyclic amino group were tested. This modification would, in addition, abolish the interaction of the adenosine derivatives with adenosine receptors.[19] Various combinations were tried, N^6-benzyl,N^6-methyl-substitution (**3**, PSB-12437) yielding the best results (**Table 1**).

The co-crystal structure of **2** indicates a pocket next to the adenine base with a volume of ≈210 Å^3. This pocket has a mostly polar surface formed by N390, D524, NH^{F417}, NH^{F500}, and CO^{G393}, and a hydrophobic base formed by the side chains of F412, P498, L415, L389, and I364. Since this pocket is expected to be best accessible via substitution at the C2-position of the adenine nucleobase, we synthesized 2-substituted AOPCP derivatives exploring this modification to enhance the inhibitory potency. Various substituents were tried, but only halogens (chloro and iodo) resulted in (similarly) improved inhibitory activity. Therefore, we combined the N^6-benzyl group of inhibitor **2** with a 2-chloro substituent resulting in the very potent inhibitor **4** (PSB-12651, Table 1). Finally, the optimized inhibitor **5** (PSB-12489) was designed by combining the improved features of both inhibitors **3** and **4** (**Figure 2**). The resulting compound **5** (Table 1), a hybrid of **3** and **4**, in fact showed increased potency as predicted based on the X-ray co-crystal structure of inhibitor **2** with CD73.

For the preparation of the target compounds **3–5**, a convergent synthetic strategy[17] was applied, which involved the synthesis of the intermediate nucleosides **6–8** followed by phosphonylation to the desired nucleotide analogs (**Scheme 1**). Inosine (**9a**) and guanosine (**9b**) were acetylated with acetic anhydride to yield 2′,3′,5′-*O*-acetyl-inosine (**10a**) and -guanosine (**10b**). Chlorination in position 6 yielded **11a-b**. Intermediate **11a** was treated with *N*-methyl-1-phenylmethanamine followed by acetyl deprotection resulting in nucleoside **6**. Compound **11b** was diazotized[20] using benzyltriethylammonium nitrite followed by reaction with acetyl chloride to furnish 2′,3′,5′-*O*-acetyl-2,6-dichloropurine riboside (**12**). Intermediate **12** was reacted with benzylamine or with *N*-methyl-1-phenylmethanamine followed by acetyl deprotection resulting in nucleosides **7** and **8**. Reaction of nucleosides **6–8** with methylenebis(phosphonic dichloride)[17] followed by hydrolysis with triethylammonium chloride (TEAC) yielded the final nucleotides **3–5**. The products were obtained in overall yields of 30–35% (Scheme 1).

The synthesis of 2′,3′,5′-*O*-acetyl-2,6-dichloropurine riboside (**12**) from guanosine (**9b**), a precursor for the potent inhibitor **5**, requires a tedious five-step procedure. Since **5** was required in gram amounts for biological studies, we upscaled its

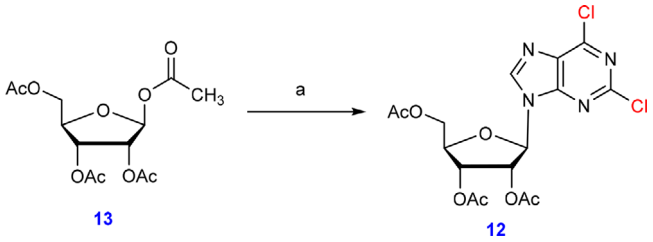

Scheme 2. Improved synthesis of 2′,3′,5′-*O*-acetyl-2,6-dichloropurine riboside. Reagents and conditions: a) 2,6-dichloropurine, trifluoromethanesulfonic acid, 85 °C, 1 h, yield 69%. For detailed synthetic procedure, see Supporting Information.

synthesis, and for this purpose, the synthetic access to nucleoside **12** was significantly improved.[21] This key compound was obtained in a single step by reaction of tetraacetylribose (**13**) with 2,6-dichloropurine in the presence of trifluoromethanesulfonic acid affording **12** in high yield and purity after simple crystallization (**Scheme 2**). Compound **5** was thus obtained in 45–50% overall yield.

The CD73-inhibitory potency of the new compounds was initially determined using recombinant soluble rat CD73 expressed in Sf9 insect cells[22] via a sensitive radiometric assay which allows the use of substrate concentrations around the low K_m value of CD73.[23] Full concentration–response curves were determined, and K_i values were calculated from the obtained IC_{50} values using the Cheng–Prusoff equation (see Table 1 and Figure S4, Supporting Information).[24] The CD73 inhibitors ADP, **1** and **2** had previously been characterized in the same assay showing K_i values of 3880, 197, and 9.03 nM, respectively.[17] The new inhibitors **3** and **4** displayed improved K_i values of 4.64 and 1.23 nM, respectively. The hybrid inhibitor **5** having the N^6-benzyl-N^6-methyl disubstitution of **3** combined with 2-chloro substitution as in **4** resulted in the first subnanomolar CD73 inhibitor showing a K_i value of 0.746 nM, which corresponds to a 264-fold improvement in potency as compared to the standard CD73 inhibitor AOPCP (**1**).

Subsequently, the most potent inhibitor **5** was broadly investigated. When tested at human recombinant soluble CD73 in a radiometric assay,[25] it displayed an even lower K_i value of 0.318 nM as compared to the rat enzyme (see Table 1 and **Figure 3**). Native human serum CD73[26] was also potently inhibited by **5** with a K_i value of 2.51 nM (as compared to a K_i value of 487 nM determined for AOPCP) (Figure 3).

In vivo, CD73 is known to be present in soluble as well as in membrane-bound form. Thus, we studied inhibition of natively expressed CD73 in a human breast cancer cell line, MDA-MB-231, and in human umbilical vein endothelial cells (HUVECs) by compound **5** in comparison to **1** (see Figure 3) using the same assay.[25] The IC_{50} value of **5** was 104 nM in MDA-MB-231 cells and 73.5 nM in HUVEC cells, corresponding to K_i values of 3–5 nM, while that for **1** was determined to be 150–200 nM. Inhibitor **5** was additionally tested at several other CD73-expressing cell lines. In all experiments, concentration-dependent inhibition of CD73 was observed with similar high potencies (see Figure S6, Supporting Information).

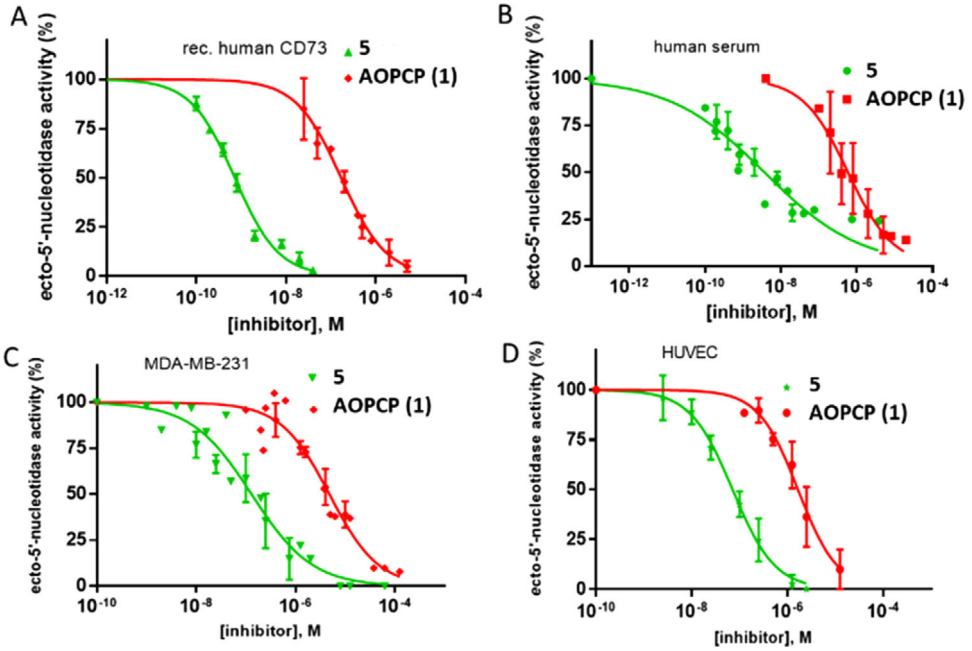

Figure 3. Concentration-dependent inhibition of different preparations of human CD73 by the standard inhibitor **1** and the new inhibitor **5**. A) Soluble human recombinant CD73 (K_m 40 μM), K_i 88.4 nM for **1**, 0.318 nM for **5**. B) Native soluble CD73 in human serum (K_m 65 μM), K_i 487 nM for **1**, 2.51 nM for **5**. C) Human breast cancer cells, IC_{50} 5720 nM for **1**, 104 nM for **5** (substrate concentration: 400 μM AMP). D) HUVEC cells, IC_{50} 1860 nM for **1**, 73.5 nM for **5** (substrate concentration: 200 μM AMP). Concentration–inhibition curves were performed in 2–4 separate experiments in duplicates, and the results are presented as mean ± standard deviation (SD). K_i values were calculated from the obtained IC_{50} values by using the Cheng–Prusoff equation. For complete results see Table S2, Supporting Information. For comparison, inhibition constants of **1** and **5** at the recombinant human enzyme have also been determined by Michaelis–Menten plots, and the results, which are in the same range, are presented in Figure S5, Supporting Information.

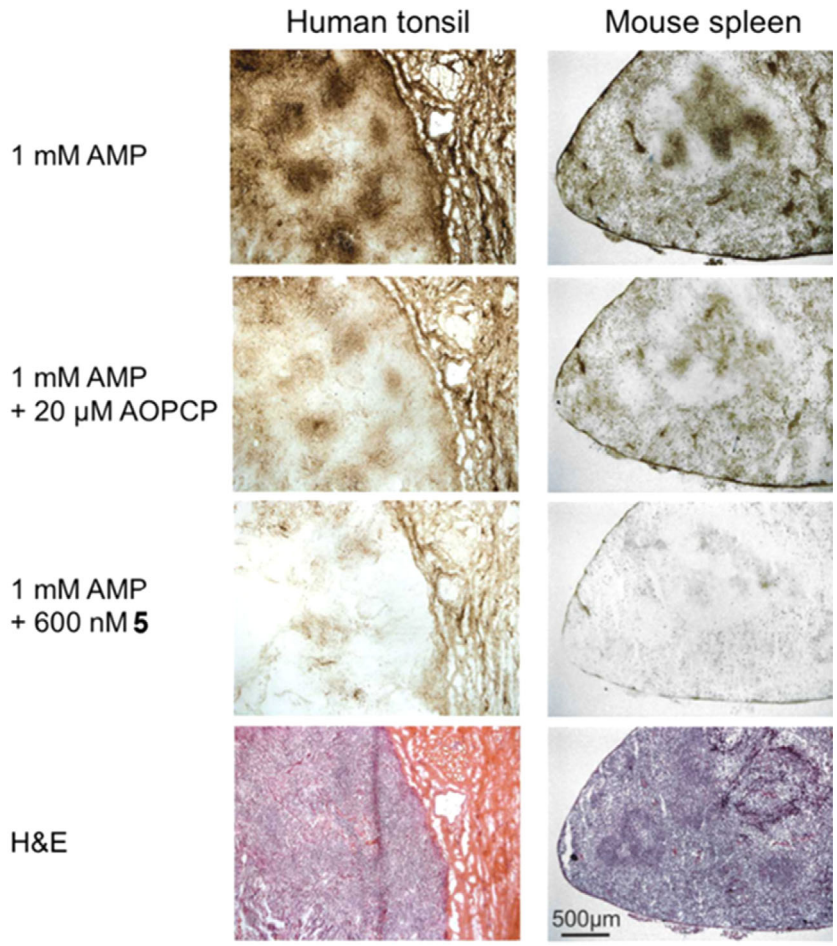

Figure 4. Enzyme histochemical staining of human tonsil and mouse spleen tissue section. CD73 substrate AMP (1 mM) was added in the absence or presence of the standard inhibitor AOPCP (**1**, 20 μM) or **5** (600 nM). On the lower panel, the tissue sections were stained with hematoxylin and eosin (H&E) for visualization of tissue structures. Inhibitor **5** blocked CD73 activity at a concentration of 600 nM and was significantly more efficient than the standard inhibitor **1** utilized at a higher concentration of 20 μM as shown by reduced brown staining.

To go one step further, we tested CD73 inhibition by compound **5** in mouse and human tissues. We utilized human tonsil and mouse spleen sections since both of these tissues are known to express CD73.[26] To this end, the $Pb(NO_3)_2$ staining technique was used for the detection of phosphate as a product of CD73-mediated AMP hydrolysis resulting in the precipitation of $Pb_3(PO_4)_2$. After wash-out of excess $Pb(NO_3)_2$, $(NH_4)_2S$ was added resulting in PbS precipitation, which is detectable as brown precipitation.[26] Human tonsils and mouse spleen tissue sections were incubated with 1 mM AMP in the absence or presence of 20 μM AOPCP, or 600 nM of **5** (and also with hematoxylin/eosin dyes to distinguish different tissue structures). Especially in the regions of the central arteries and the capsule, intensive brown staining—corresponding to high CD73 activity—was observed in both tissues. This activity was clearly reduced in the inhibitor-treated samples. Inhibitor **5** was significantly more potent and efficacious than **1** as shown by reduced brown staining (**Figure 4**). In fact, inhibitor **5** was identified as the most potent CD73 inhibitor observed so far also in this type of assay.

Next, we determined the binding mode of inhibitor **5** to human CD73 by X-ray analysis to understand the basis of its outstanding potency. The chlorine atom at C2 forms a hydrogen bond with the N390 side chain and with a water molecule coordinated to CO^{N499} (Figure 1). Both donors are perfectly positioned in a side-on orientation. Furthermore, two CH-groups are positioned to interact with the chloro substituent, which thus has a very favorable environment for biomolecular interactions.[27] The Cl substituent is not involved in halogen bonding interactions as the carbonyl oxygen of N390 as the only nearby interaction partner is not positioned for a favorable halogen bond. The C—Cl···O angle deviates too much from linearity (Figure 1D).[28] The presence of the Cl-substituent in **5** also causes a relocation of a water molecule in the C2 pocket to an adjacent previously unoccupied binding site. Taken together, the chloro substitution at C2 results in overall more favorable interactions in the C2 pocket explaining the increase in inhibitory potency.

A comparison of the binding modes of **2** and **5** shows that the common AOPCP core structures superimpose closely, but the N^6-benzyl substituents differ by 37.8° in their torsion angle around the bond between N^6 and the methylene carbon of the benzyl group (Figure 1A). This moderate reorientation of the phenyl ring is in line with the generally somewhat flexible

interaction of this group with the N-terminal domain, which is also apparent in the co-crystal structure of **5** by the weaker electron density of this group. The reorientation may be caused by the presence of the N^6 methyl group in **5** and/or by a slight 0.3 Å shift of the adenine ring of **5** compared to **2** toward the C2 pocket.

As a next step, we investigated the selectivity of inhibitor **5** for CD73 versus related targets. Inhibition of other important ectonucleotidases, including the ectonucleoside triphosphate diphosphohydrolases (NTPDases) 1–3 and the nucleotide pyrophosphatases/phosphodiesterases (NPPs) 1–3, was investigated according to described procedures.[13] The standard CD73 inhibitor **1** was previously found to additionally inhibit NPP1.[17] The new inhibitor **5** did not inhibit any of these ectonucleotidases nor did it activate or inhibit any of the ADP-activated P2 receptors, $P2Y_1$ and $P2Y_{12}$, at a concentration of 10 μM (see Tables S3 and S4, Supporting Information).

Finally, inhibitor **5** was further investigated for its stability in human blood plasma and in rat liver microsomes. Known CD73 inhibitors (ADP, **1**, and **2**) were included for comparison. The experiments were performed as previously described[17] incubating the samples at 37 °C and analyzing them by LC-MS. In human blood plasma, **5** was completely stable within the incubation period of 5 h. Compound **2** was less stable (8% degradation), **1** was metabolized by approximately 50%, while ADP was completely degraded within 30 min. Thus, the order of stability in human blood plasma was **5** ≥ **2** > **1** ≫ ADP (see Figure S7, Supporting Information). Incubation with rat liver microsomes demonstrated that **5** is metabolically highly stable. Only less than 5% were metabolized under the applied conditions after incubation for 8 h. Inhibitor **2** was less stable (25% degradation), while ADP and **1** were completely degraded within 5–15 min. Thus, the order of stability in rat liver microsomes was **5** > **2** ≫ **1** > ADP (for details see Figure S7, Supporting Information).

In conclusion, we obtained an X-ray co-crystal structure of human ecto-5'-nucleotidase (CD73) in complex with inhibitor **2**, which allowed us to design nucleotide analogue **5**. The new CD73 inhibitor **5** shows outstanding potency, selectivity, and metabolic stability, with a subnanomolar K_i value at the human and the rat enzyme. Compound **5** is the most potent CD73 inhibitor described to date as demonstrated for recombinant CD73 as well as for native CD73-containing preparations including soluble enzyme in blood plasma, and membrane-bound CD73 in epithelial and cancer cells, and in mouse and human tissue sections. Importantly, for **5** there is no risk of the formation of adenosine receptor-activating compounds, which could lead to serious side effects. Therefore, **5** is an excellent tool compound for in vitro and in vivo studies. Based on our results, the first clinical candidate (AB680, see Figure S10, Supporting Information) has recently been announced.[29,30] Small molecule CD73 inhibitors are novel check-point inhibitors, which are expected to be superior to antibodies for the immunotherapy of cancer.

[Final coordinates and structure factors of co-crystals with inhibitors PSB-12379 (**2**) and PSB-12489 (**5**) have been deposited in the Protein Data Bank (www.rcsb.org) under the accession codes 6s7f and 6s7h].

Supporting Information

Supporting Information is available from the Wiley Online Library or from the author.

Acknowledgements

S.B. and J.P. contributed equally to this work. S.B. and C.E.M. were supported by the Ministry for Innovation, Science, Research and Technology of the State of North-Rhine-Westfalia (NRW International Graduate Research School BIOTECH-PHARMA). This work was also supported by the Deutsche Forschungsgemeinschaft (Grant Numbers: SFB1052, SFB1328). The authors thank Marion Schneider for LCMS analyses, and Sabine Terhart-Krabbe and Annette Reiner for NMR spectra. Dr. Mikael Maksimow, Turku, Finland, is acknowledged for providing human recombinant CD73. G.G.Y. thanks Prof. Sirpa Jalkanen for helpful advice. N.S. and J.P. thank the SFB 1052 for support. J.P. and N.S. are grateful to the Joint Berlin MX-Laboratory at BESSY II, Berlin, Germany, for beam time and assistance during synchrotron data collection and to the Helmholtz Zentrum Berlin for traveling support.

Conflict of Interest

N.S. and C.E.M. have given scientific advice to Arcus Biosciences.

Keywords

cancer, CD73 inhibitors, immunotherapy, nucleotide analogs, X-ray co-crystal structures

Received: May 21, 2019
Revised: July 5, 2019
Published online: July 31, 2019

[1] L. Antonioli, M. Fornai, C. Blandizzi, P. Pacher, G. Haskó, *Immunol. Lett.* **2019**, *205*, 9.
[2] D. Vijayan, A. Young, M. W. L. Teng, M. J. Smyth, *Nat. Rev. Cancer* **2017**, *17*, 709.
[3] H. Zimmermann, M. Zebisch, N. Sträter, *Purinergic Signal.* **2012**, *8*, 437.
[4] G. G. Yegutkin, *Crit. Rev. Biochem. Mol. Biol.* **2014**, *49*, 473.
[5] K. Knapp, M. Zebisch, J. Pippel, A. El-Tayeb, C. E. Müller, N. Sträter, *Structure* **2012**, *20*, 2161.
[6] B. Allard, M. S. Longhi, S. C. Robson, J. Stagg, *Immunol. Rev.* **2017**, *276*, 121.
[7] B. Zhang, *Cancer Res.* **2010**, *70*, 6407.
[8] C. M. Hay, E. Sult, Q. Huang, K. Mulgrew, S. R. Fuhrmann, K. A. McGlinchey, S. A. Hammond, R. Rothstein, J. Rios-Doria, E. Poon, N. Holoweckyj, N. M. Durham, C. C. Leow, G. Diedrich, M. Damschroder, R. Herbst, R. E. Hollingsworth, K. F. Sachsenmeier, *OncoImmunology* **2016**, *5*, e1208875.
[9] Y. Baqi, S.-Y. Lee, J. Iqbal, P. Ripphausen, A. Lehr, A. B. Scheiff, H. Zimmermann, J. Bajorath, C. E. Müller, *J. Med. Chem.* **2010**, *53*, 2076.
[10] P. Ripphausen, M. Freundlieb, A. Brunschweiger, H. Zimmermann, C. E. Müller, J. Bajorath, *J. Med. Chem.* **2012**, *55*, 6576.
[11] R. Raza, A. Saeed, J. Lecka, J. Sévigny, J. Iqbal, *Med. Chem.* **2012**, *6*, 1133.
[12] J. Iqbal, A. Saeed, R. Raza, A. Matin, A. Hameed, N. Furtmann, J. Lecka, J. Sévigny, J. Bajorath, *Eur. J. Med. Chem.* **2013**, *70*, 685.

[13] S.-Y. Lee, A. Fiene, W. Li, T. Hanck, K. A. Brylev, V. E. Fedorov, J. Lecka, A. Haider, H. J. Pietzsch, H. Zimmermann, J. Sévigny, U. Kortz, H. Stephan, C. E. Müller, *Biochem. Pharmacol.* **2015**, *93*, 171.
[14] P. F. Corbelini, F. Figueiró, G. M. Das-Neves, S. Andrade, D. F. Kawano, A. M. Oliveira-Battastini, V. L. Eifler-Lima, *Curr. Med. Chem.* **2015**, *15*, 1776.
[15] C. Dumontet, S. Peyrottes, C. Rabeson, E. Cros-Perrial, P. Y. Géant, L. Chaloin, L. P. Jordheim, *Eur. J. Med. Chem.* **2018**, *157*, 1051.
[16] X. Liu, M. Wright, C. E. Hop, *J. Med. Chem.* **2014**, *57*, 8238.
[17] S. Bhattarai, M. Freundlieb, J. Pippel, A. Meyer, A. Abdelrahman, A. Fiene, S.-Y. Lee, H. Zimmermann, G. G. Yegutkin, N. Sträter, A. El-Tayeb, C. E. Müller, *J. Med. Chem.* **2015**, *58*, 6248.
[18] A. Junker, C. Renn, C. Dobelmann, V. Namasivayam, S. Jain, K. Losenkova, H. Irjala, S. Duca, R. Balasubramanian, S. Chakraborty, F. Börgel, H. Zimmermann, G. G. Yegutkin, C. E. Müller, K. A. Jacobson, *J. Med. Chem.* **2019**, *62*, 3677.
[19] C. E. Müller, K. A. Jacobson, *Biochim. Biophys. Acta, Biomembr.* **2011**, *5*, 1290.
[20] P. Francom, Z. Janeba, S. Shibuya, M. J. Robins, *J. Org. Chem.* **2002**, *67*, 6788.
[21] *Nucleic Acids in Chemistry and Biology* (Eds: G. Blackburn, M. Gait, D. Loakes, D. Williams), 3rd ed., Royal Society of Chemistry, London **2015**, Ch. 3.
[22] J. Servos, H. Reiländer, H. Zimmermann, *Drug Dev. Res.* **1998**, *45*, 269.
[23] M. Freundlieb, H. Zimmermann, C. E. Müller, *Anal. Biochem.* **2014**, *446*, 53.
[24] Y.-C. Cheng, W. H. Prusoff, *Biochem. Pharmacol.* **1973**, *22*, 3099.
[25] G. G. Yegutkin, S. S. Samburski, S. Jalkanen, *FASEB J.* **2003**, *17*, 1328.
[26] G. G. Yegutkin, K. Auvinen, M. Karikoski, P. Rantakari, H. Gerke, K. Elima, M. Maksimow, I. B. Quintero, P. Vihko, M. Salmi, S. Jalkanen, *Mediators Inflamm.* **2014**, *2014*, 485743.
[27] Y. Lu, Y. Wang, Z. Xu, X. Yan, X. Luo, H. Jiang, W. Zhu, *J. Phys. Chem. B* **2009**, *113*, 12615.
[28] R. Wilcken, M. O. Zimmermann, A. Lange, A. C. Joerger, F. M. Boeckler, *J. Med. Chem.* **2013**, *56*, 41363.
[29] Arcus Biosciences Inc, WO2017120508, **2017**.
[30] T. Nguyen, Drug structures displayed for the first time in Orlando, https://cen.acs.org/pharmaceuticals/drug-discovery/Drug-structures-displayed-first-time-in-Orlando/97/web/2019/04 (accessed: May 2019).